Femtosecond laser ablation of dielectric materials in the optical breakdown regime: Expansion of a transparent shell

M. Garcia-Lechuga, J. Siegel, J. Hernandez-Rueda, and J. Solis

Femtosecond laser ablation of dielectric materials in the optical breakdown regime: Expansion of a transparent shell

M. Garcia-Lechuga, J. Siegel,[a)] J. Hernandez-Rueda, and J. Solis
Laser Processing Group, Instituto de Optica, Serrano 121, 28006 Madrid, Spain

Phase transition pathways of matter upon ablation with ultrashort laser pulses have been considered to be understood long-since for metals and semiconductors. We provide evidence that also certain dielectrics follow the same pathway, even at high pulse energies triggering optical breakdown. Employing femtosecond microscopy, we observe a characteristic ring pattern within the ablating region that dynamically changes for increasing time delays between pump and probe pulse. These *transient Newton rings* are related to optical interference of the probe beam reflected at the front surface of the ablating layer with the reflection at the interface of the non-ablating substrate. Analysis of the ring structure shows that the ablation mechanism is initiated by a rarefaction wave leading within a few tens of picoseconds to the formation of a transparent thin shell of reduced density and refractive index, featuring optically sharp interfaces. The shell expands and eventually detaches from the solid material at delays of the order of 100 ps. © *2014 AIP Publishing LLC*.
[http://dx.doi.org/10.1063/1.4895926]

Ultrashort laser pulses have the ability to generate extreme excitation levels in matter and trigger processes that would not be achievable with other methods. These include a broad range of non-linear effects and non-equilibrium phase transitions, which are of great interest for fundamental physics and straight-forward technological applications.[1] The pulse intensity regime above the damage threshold is of particular interest for modern laser micromachining and nanostructuring strategies;[2] although the underlying modification pathways and dynamics become highly complex, especially when material removal (ablation) is involved. In this field, the work by Sokolowski-Tinten and co-workers on the ablation dynamics of metals and semiconductors[3] meant an important leap forward in the comprehension of the underlying mechanisms. The authors discovered an optical interference phenomenon in the nanosecond delay range, so-called transient Newton rings that rapidly change their period with time, which provided the basis for understanding the ablation dynamics. The nanometer thickness resolution of the technique has been demonstrated recently in a study of an evaporating water droplet, although with a low temporal resolution (milliseconds).[4]

The scenario for semiconductors and metals, deduced from those studies and supported by theoretical calculations, is that a thin layer experiences isochoric heating to temperatures above the critical temperature to form a hot fluid at solid density. The subsequent adiabatic expansion can be described by a rarefaction wave travelling into the material and leaving behind a two-phase region of liquid-gas coexistence. The strong decrease of the speed of sound at the border of this region and the reflection of the rarefaction wave at the liquid-solid interface are responsible for the formation of two sharp interfaces, necessary for observing interference effects.[3,5]

While transient Newton rings are considered to be a universal phenomenon in the ablation process of metals and semiconductors (observed in Au, Al, Ti, Pt, Cu, Ni, Cr, Mg, Hg, GeSb, Ge, C, GaAs, InP, and Si),[3,5–9] such rings have never been observed in dielectrics, despite several works reporting on the ablation dynamics of different dielectrics (BK7 glass, fused silica, and quartz).[6,7,10,11] This absence has been attributed to a fundamentally different ablation process taking place in these materials, triggered by multi-photon and impact ionization that eventually lead to optical breakdown with an extremely high degree of ionization,[12–14] as opposed to linear or few-photon absorption processes.

In the present work we report the observation of transient Newton rings in three dielectrics, namely, sapphire and lithium niobate, as representatives of crystalline materials, and a high refractive index glass. We discuss the differences to Newton rings in metals and semiconductors and point out possible reasons why these rings have not been previously observed. Their mere existence has important consequences for the comprehension of the ablation process in dielectrics, being essentially the same, within a certain fluence regime, as in semiconductors and metals. An analysis of the fringe pattern allows a determination of the expansion velocities of the ablating shell. Combined with modeling of the reflectivity changes, the transient optical properties of the shell structure can be estimated for the different stages of the ablation process.

For our study, we have employed femtosecond-resolved microscopy[8,15] upon irradiation with single s-polarized 120 fs pulses at 800 nm, focused onto the sample surface at an angle of 53°, producing an elliptical excitation spot with a Gaussian intensity distribution (98.4 μm $\times$ 59.0 μm 1/e^2 diameters). The probe pulse is frequency-doubled with a Beta Barium Borate crystal to 400 nm and delayed with respect to the pump pulse by an optical delay line. The probe light reflected from the sample surface is imaged with an objective lens (80$\times$, NA 0.45) and a tube lens onto the chip

a)Author to whom correspondence should be addressed. Electronic mail: j.siegel@io.cfmac.csic.es

of a 12-bit charge-coupled device (CCD) camera. The effective temporal resolution of the setup has been optimized to be approximately $\leq$200 fs, using a prism compressor.

The samples studied were sapphire (crystalline Al_2O_3) from VM-TIM Germany with an optical bandgap of 9.9 eV, undoped lithium niobate ($LiNbO_3$) from VM-TIM with a bandgap of 3.5 eV, and commercial glass from Schott (SF57) with a composition of 59·SiO_2–40·PbO–1·Na_2O molar %, and an optical bandgap of 3.2 eV.

Figures 1(a)–1(c) show time-resolved optical micrographs of the surface of the three samples studied, recorded at time delays of a few hundred picoseconds after exposure to single laser pulses at fluences above the ablation threshold. In all cases, a pattern of alternating bright and dark rings with a central disk is observed, very similar to the transient Newton rings observed in semiconductors and metals.[3] While fs pump-probe techniques have not been used previously on $LiNbO_3$ and SF57 for studying their ablation dynamics, they have been used on sapphire. Yet, none of the works has reported the observation of transient Newton rings during the ablation process, neither in their direct 2D manifestation (when using fs microscopy), nor in form of oscillations (when using point probing).[11,16–18]

In order to demonstrate that ring appearance is related to ablation, we have performed measurements of the sample topography after irradiation. Fig. 1(d) shows the crater profile corresponding to the image shown in Fig. 1(a) for $LiNbO_3$. A good match of the crater diameter to the spatial extension of the ring system is found. This also holds for the other materials studied (not shown).

An obvious verification of the interference-nature of the rings that can be performed in transparent materials is the acquisition of images in reflection and transmission. As illustrated in Fig. 1(e), interference effects in reflection necessarily lead to corresponding effects in transmission. In order to avoid image degradation by spherical aberration when imaging through the sample, we kept the microscope/irradiation configuration unchanged for transmission measurements, but sent instead the probe pulse from behind, through the sample. Fig. 1(f) shows the corresponding micrographs recorded at 400 ps delay, at slightly higher peak fluence than used in Fig. 1(a). In both cases a ring pattern can

be observed, confirming that these are indeed Newton rings. The ring pattern is of opposite sign as expected, i.e., an interference maximum in reflection corresponds to a minimum in transmission, which can easily be appreciated by looking at the central disk.

The above results imply that two conditions are met in the ablation process in dielectrics, which form the fundamental requirements for the formation of Newton rings: First, the existence of two optically flat interfaces (the ablation front and the interface of the ablating layer with the solid material). Second, a considerable refractive index difference at the probe wavelength between the non-exited material ($n_{LiNbO3} = 2.44$, $n_{SF57} = 1.92$, $n_{Al2O3} = 1.79$) and the effective refractive index n_{eff} of the ablating layer, combined with a relatively low absorption coefficient k_{eff}, thus enabling interference without too strong attenuation. As for the first requirement, traditionally it has been assumed that for dielectrics the sharp transition from almost no excitation to very strong excitation, leading to the formation of a highly ionized plasma, prevented the phase decomposition scenario described in Ref. 3 in which the expansion isentrope passes through the liquid-gas coexistence regime. Yet, there is no fundamental reason why this regime should not exist in dielectrics just as in metals/semiconductors, although the non-linear absorption process in the former poses a challenge on generating the necessary experimental conditions for passing the liquid-gas coexistence regime. Our observation of transient Newton rings in dielectrics implies that there is indeed a fluence interval where these conditions can be achieved, leading to an ablation behavior that is essentially similar to that of non-dielectric materials.

The fulfillment of the second requirement is also challenging. Starting from an already low refractive index, compared to that of semiconductors, a further lowering (by rarefaction, a reduction in density due to expansion of the shell) will be relatively small, leading to a relatively small optical contrast. Also, the requirement of a low absorption coefficient is not trivial to accomplish due to the highly ionized state of the ablating matter after optical breakdown. Yet, as shown by the data in Fig. 1, both conditions are met in the studied materials sufficiently well to produce Newton rings with an optical contrast (OC = $(R_{max} − R_{min})/R_{material}$)
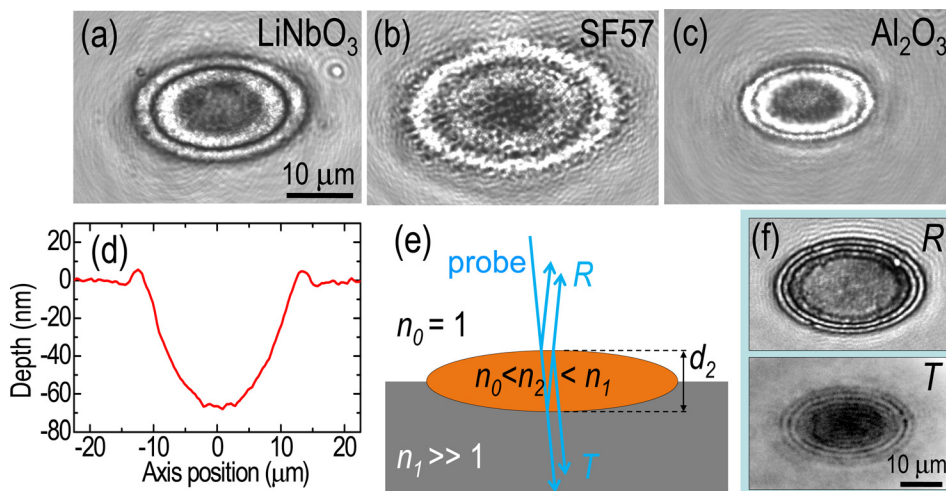
FIG. 1. (a)–(c) Time-resolved optical micrographs of laser-irradiated dielectrics recorded with sub-nanosecond time delays ($LiNbO_3$ at 315 ps, SF57 at 415 ps, and sapphire at 215 ps), featuring transient Newton rings. (d) Final ablation crater profile for the irradiation shown in (a). (e) Sketch of the scenario of an ablating layer of lower refractive index n_2 compared to the one of the bulk n_1. (f) Comparison of the appearance of transient Newton rings in reflection (R) and transmission (T) for $LiNbO_3$ at 400 ps delay. For the transmission micrograph, the contrast has been enhanced in order to reveal the ring structure.

of $OC_{LiNbO3} = 1.3$, $OC_{SF57} = 1.8$, $OC_{Al2O3} = 1.8$. These strong constraints are the most likely reasons for transient Newton rings not having been observed so far, or overlooked.

For a detailed study of the temporal evolution of the Newton rings, we have chosen the case of $LiNbO_3$, since their visibility throughout the entire optical delay studied is highest compared to the other materials, most likely due to the very high initial refractive index. Figure 2 shows a sequence of snap-shots of the ablation process at different temporal delays of the probe pulse after the arrival of the pump pulse with a fluence $F_{peak} = 2.0 \, J/cm^2$. Optical breakdown occurs as can be seen by the formation of a highly reflective dense free-electron plasma within less than 1 ps after the pump pulse. At 10 ps, the highly ionized state of the material can be appreciated by the very low reflectivity in the central region. The surrounding ring of slightly higher reflectivity corresponds to a free electron plasma induced at lower local fluence, which has not yet fully relaxed.[11] Already at $t = 35$ ps delay, the formation of the first Newton ring feature can be observed, a dark ring (interference minimum) and a slightly brighter inner disk (maximum). The number of rings continuously increases with delay at the expense of ring width, consistently with the increase of the thickness d_2 of the expanding ablation layer. At the highest delay studied (895 ps), along with the Newton rings inside the ablation crater, diffraction rings are observed outside the crater region.[11] The lower fluence threshold for the appearance of Newton rings in this material, equal to the ablation threshold, is $F_{th,low} = 1.55 \, J/cm^2$. The upper threshold, above which the expansion isentrope no longer passes through the two-phase region, is $F_{th,high} = 2.05 \, J/cm^2$, which we have determined separately in an experiment performed at higher fluence.

The transient optical thickness $n_2 \times d_2$ and shape of the ablation layer can be determined by measuring for each image the spatial position of intensity maxima and minima.

This has been done in the lower left graph in Fig. 2, providing a visual representation of the expansion of ablation front. As reported for semiconductors and metals,[6] the shape of the curves follows a Gaussian function.

The position of the ablation front center as a function of delay time is shown in the right graph in Fig. 2. An apparently linear dependence can be observed and a maximum "optical velocity" can be determined from the slope, yielding $v_{opt} = 1170 \, m/s$. In order to convert this value into a real velocity of the ablation front, the unknown effective refractive index n_2 of the ablating layer is needed for calculating $v = v_{opt}/n_2$. Considering the basic scenario, in which the ablating layer consists of an expanded two phase liquid/gas region with a refractive index much reduced compared to the bulk material, we set $n_2 = 1.5$ and support this choice later by modeling. In this case, the velocity of the ablation front becomes $v = 780 \, m/s$, which is comparable to those obtained for semiconductors and metals.[6]

An estimation can also be made for the arrival time of the rarefaction wave at the boundary with the non-ablating material at $t = d/c_0$, with d being the ablation depth ($d = 70$ nm, c.f. Fig. 1(d)) and c_0 being the sound velocity. Since the expanding material is in a fluid state, the sound velocity can be much lower than for the solid material. Following Ref. 3 we use $c_0 = 2.5 \, km/s$ and obtain $t = 28$ ps for the arrival time of the rarefaction wave. Within the hydrodynamic model that is typically applied to such an ablation scenario in semiconductors and metals,[19] the wave is reflected upon arrival, leading to a further decrease of the density near the substrate. The reflected wave travels at approximately the same speed and in the same direction as the ablation front, leading to the formation of a structure composed of a thin shell enclosing a low density volume, whose density is continuously reduced as the shell expands further.[5,20,21] According to this model, the transition from a homogeneous plume to a shell structure should occur essentially at the moment when the rarefaction wave is reflected.
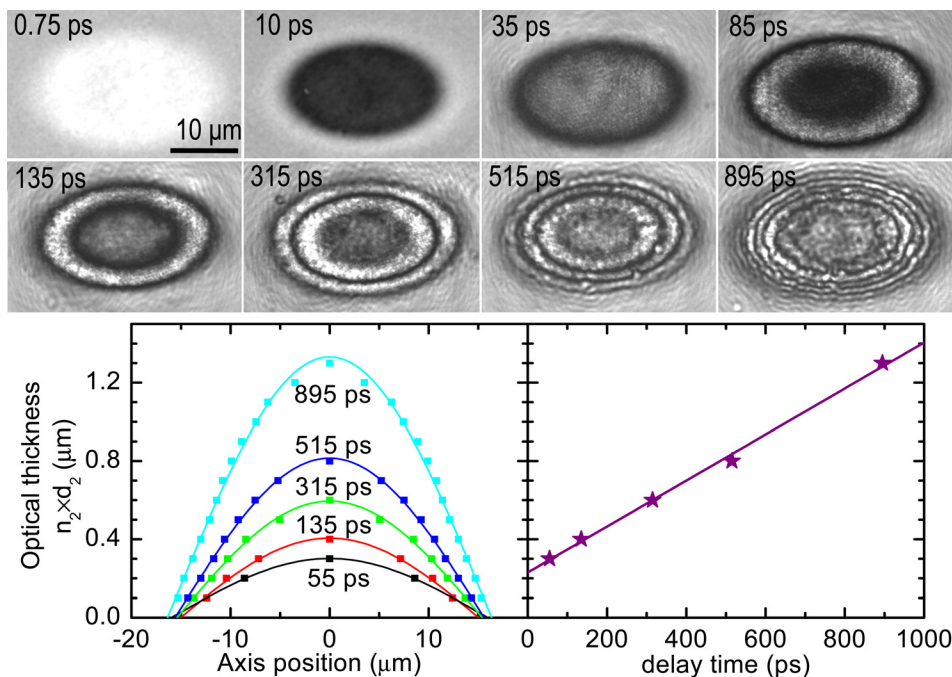
FIG. 2. Top: Temporal evolution of the surface reflectivity of $LiNbO_3$ after laser irradiation, featuring optical breakdown followed by ablation and formation of transient Newton rings. The pump-probe delay times are indicated in each frame. Bottom left: Optical thickness of the ablating layer as a function of the horizontal axis position within the spot, as extracted from the above images. The data points are experimental data, the lines are fits to a Gaussian distribution Bottom right: Optical thickness of the ablating layer at the spot center as a function of delay.

An important question remains: Can the two regimes be distinguished experimentally and their transition determined? We have investigated this question by implementing a model based on the theory of Abeles for calculating optical effects in multilayer systems.[22] In the model, the first scenario considered is the one of a homogeneous plume shown in Fig. 3(c), a bilayer system consisting of a thin ablating layer with modified optical constants (n_2, k_2) and thickness d_2 on top of an infinite bulk material (n_1). The reflectivity is then calculated as a function of d_2 (maximum transformed layer thickness). The aim of this calculation is reproducing the number of Newton rings and their optical contrast. For that purpose, reflectivity profiles of the transient images have been extracted and used as target for the simulation. By counting the number of rings (reflectivity maxima and minima) a first guess value of d_2 can be obtained. Subsequently, the optical constants n_2 and k_2 are adjusted iteratively in order to obtain the best match with the modulation amplitude, its sign with respect to the initial reflectivity R_0, and possible damping. The second scenario considered is the one of a "bubble" structure shown in Fig. 3(d), composed of a dense shell with n_2, k_2 enclosing a low density region with n_3, k_3. The optical properties and layer thickness retrieved have been tested for fulfilling to a reasonable extent ($\pm 20\%$, considering the simplicity of the model) the mass conservation condition. We assume that the ablated mass is proportional to the ablation depth d and related to refractive index as $(n_1 - 1) \times d = (n_2 - 1) \times d_2 + (n_3 - 1) \times d_3$.

We have applied this model with the two possible scenarios to study two cases. First, the Newton rings recorded at a delay of $t = 35$ ps, which is very close to the expected transition. Figure 3(a) shows the reflectivity profile at $t = 35$ ps together with the simulation result, showing the best match in terms of amplitude, sign, and thickness for the homogeneous plume model with $n_2 = 1.7 \pm 0.1$ and $k_2 = 0.20 \pm 0.05$. Higher values of n_2 would lead to a lower modulation amplitude than observed experimentally. The elevated value of k_2 takes account of the modulation damping towards the spot

center (we have confirmed that the reflectivity value in the center is an actual Newton interference maximum by verifying that at a delay of 55 ps the reflectivity in the center decreases). The limited *spatial* coincidence of the calculation with the experimental data on the horizontal axis is due to the Gaussian relation between axis position (bottom axis) and layer thickness (upper axis) (c.f. Fig. 2, bottom left). All attempts to fit the data to the shell model yielded results in which the shell and the enclosed volume had almost equal optical properties. This suggests that at a delay of $t = 35$ ps, the transition has not yet been reached.

The second case studied was at a much longer delay of $t = 315$ ps (c.f. Fig. 3(b)). Here, we failed to obtain a match using the scenario shown in Fig. 3(c). No combination of n_2, and k_2 provided a reflectivity increase above R_0 together with oscillations as observed experimentally. However, when using the model sketched in Fig. 3(d), the obtained fit matches well the experimental data as shown in Fig. 3(b). The obtained optical properties are $n_2 = 1.5 \pm 0.1$, $k_2 = 0.50 \pm 0.05$, and $n_3 = 1.3 \pm 0.1$, $k_3 = 0$. The outer shell is set thin enough ($d_2 = 30$ nm) to avoid internal interference yet contribute with $k_2 \neq 0$ to obtain reflectivity values above R_0. It is worth noting that Figs. 3(c) and 3(d) are true-scale instantaneous cross sections through the ablating region extracted from our measurements.

While the precision of the determined parameters is not very high due to the elevated number of fitting parameters, the results unambiguously distinguish the two different expansion scenarios. They indicate that the transition occurs later than the estimated arrival time of the rarefaction wave ($t > 28$ ps) since the data recorded at $t = 35$ ps can still be described with a homogeneous plume model. The data shown in Fig. 2 give an upper boundary of $t = 135$ ps for the transition time, since at this delay the reflectivity of the first bright ring is higher than the reflectivity of the material, which is only possible for a shell-like structure.

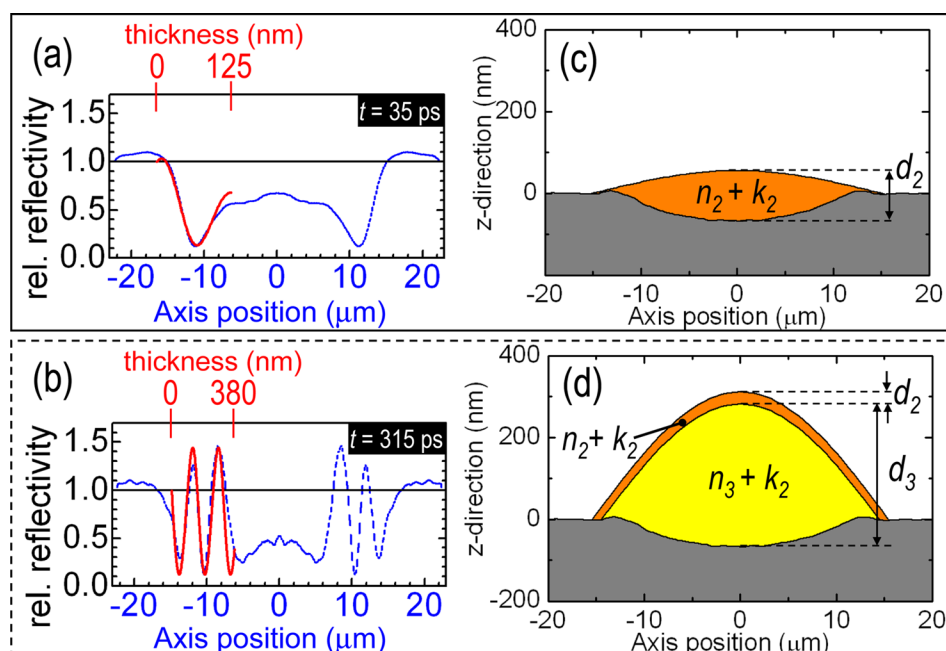Finally, we want to add an interesting detail that can be extracted from our data. The first Newton "disk"

FIG. 3. (a) and (b) Horizontal cross sections (normalized to the initial level) of the time-resolved reflectivity images at 35 ps and 315 ps delay shown in Fig. 2, respectively (blue curves). The graphs include simulated curves (red) of the relative reflectivity evolution as a function of thickness of the ablating layer. (c) and (d) True-scale instantaneous cross sections through the ablating region at the time delays corresponding to (a) and (b), respectively. The crater shape has been measured and the shape and structure of the ablating shell and its optical properties have been determined from experimental measurements in combination with modeling.

(interference minimum) should be observable when the ablating layer reaches an optical thickness $n_2 \times d_2 = \lambda/4 = 100$ nm. In view of the fact that at t = 35 ps, the first pair of Newton ring features, ring and disk, is observed, e.g., $n_2 \times d_2 = \lambda/2$, there is a possibility that the dark central region in the time-resolved image at 10 ps might actually be the first Newton "disk." This would imply that Newton rings can be observed well before the rarefaction wave reaches the non-ablating substrate indicating that the interface of the inward propagating rarefaction wave is sufficiently sharp.

In conclusion, we have observed transient Newton rings in dielectrics upon fs laser ablation, caused by interference of the probe beam reflected at the two interfaces of the transparent ablating layer. Using optical modelling we have been able to distinguish two different expansion stages, first in form of a single two-phase region and later as a thin shell enclosing a low-density region, and estimate the corresponding optical properties. As for the extracted expansion velocities we find them to be comparable to those measured for metals or semiconductors. While the present study has been limited to three selected materials with different optical and structural properties, we believe that transient Newton rings might be observable in many dielectrics (at least in those with a high refractive index) but more studies are necessary to confirm this hypothesis. These findings are highly relevant to the development of applications related to ultrafast laser structuring strategies, as they provide a means to monitor and eventually optimize the ablation dynamics in dielectrics.

[1]*Ultrashort Laser Pulse Phenomena: Fundamental, Techniques, and Applications on a Femtosecond Time Scale*, edited by J.-C. Diels and W. Rudolph (Elsevier, Amsterdam, 2014).

[2]*Femtosecond Laser Micromachining: Photonic and Microfluidic Devices in Transparent Materials*, Topics in Applied Physics Vol. 123, edited by R. Osellame, G. Cerullo, and R. Ramponi (Springer Berlin, Heidelberg, 2012).

[3]K. Sokolowski-Tinten, J. Bialkowski, A. Cavalleri, D. von der Linde, A. Oparin, J. Meyer-ter-Vehn, and S. I. Anisimov, Phys. Rev. Lett. **81**, 224 (1998).

[4]G. Verma and K. P. Singh, Appl. Phys. Lett. **104**, 244106 (2014).

[5]B. Rethfeld, V. V. Temnov, K. Sokolowski-Tinten, S. I. Anisimov, and D. von der Linde, Proc. SPIE **4760**, 72 (2002).

[6]K. Sokolowski-Tinten, J. Bialkowski, A. Cavalleri, M. Boing, H. Schüler, and D. von der Linde, Proc. SPIE **3343**, 46 (1998).

[7]D. von der Linde, K. Sokolowski-Tinten, and J. Bialkowski, Appl. Surf. Sci. **109–110**, 1 (1997).

[8]J. Bonse, G. Bachelier, and J. Siegel, J. Solid Phys. Rev. B **74**, 134106 (2006).

[9]J. Bonse, G. Bachelier, J. Siegel, J. Solis, and H. Sturm, J. Appl. Phys. **103**, 054910 (2008).

[10]J. Hernandez-Rueda, D. Puerto, J. Siegel, M. Galvan-Sosa, and J. Solid, Appl. Surf. Sci. **258**, 9389 (2012).

[11]D. Puerto, J. Siegel, W. Gawelda, M. Galvan-Sosa, L. Ehrentraut, J. Bonse, and J. Solis, J. Opt. Soc. Am. B **27**, 1065 (2010).

[12]N. M. Bulgakova, R. Stoian, A. Rosenfeld, I. V. Hertel, and E. E. B. Campbell, Phys. Rev. B **69**, 054102 (2004).

[13]B. Rethfeld, O. Brenk, N. Medvedev, H. Krutsch, and D. H. H. Hoffmann, Appl. Phys. A **101**, 19 (2010).

[14]P. Balling and J. Schou, Rep. Prog. Phys. **76**, 036502 (2013).

[15]M. C. Downer, R. L. Fork, and C. V. Shank, J. Opt. Soc. Am. B **2**, 595 (1985).

[16]I. H. Chowdhury, A. Q. Wu, X. Xu, and A. M. Weiner, Appl. Phys. A **81**, 1627 (2005).

[17]S. Guizard, N. Fedorov, A. Mouskeftaras, and S. Klimentov, AIP Conf. Proc. **1278**, 336 (2010).

[18]K. J. Wædegaard, D. B. Sandkamm, A. Mouskeftaras, and S. Guizard, Europhys. Lett. **105**, 47001 (2014).

[19]L. D. Landau and E. M. Lifshitz, *Fluid Mechanics*, Course of Theoretical Physics Vol. VII (Pergamon, Oxford, 1982).

[20]S. I. Anisimov, N. A. Inogamov, A. M. Oparin, B. Rethfeld, T. Yabe, M. Ogawa, and V. E. Fortov, Appl. Phys. A **69**, 617 (1999).

[21]V. V. Zhakhovski, K. Nishihara, S. I. Anisimov, and N. A. Inogamov, JETP Lett. **71**, 167 (2000).

[22]M. Born and E. Wolf, *Principles of Optics*, 6th ed. (Pergamon, Oxford, 1980), Sect. 1.6.